



Published in final edited form as:

Mol Cancer Ther. 2018 August ; 17(8): 1717–1726. doi:10.1158/1535-7163.MCT-17-1303.

The XPO1 inhibitor Selinexor inhibits translation and enhances the radiosensitivity of glioblastoma cells grown in vitro and in vivo

Amy Wahba, Barbara H. Rath, John W. O'Neill, Kevin Camphausen, and Philip J. Tofilon
Radiation Oncology Branch, National Cancer Institute, Bethesda, Maryland 20892

Abstract

Analysis of the radiation-induced transcriptome of glioblastoma stem-like cells (GSCs) identified an interacting network in which XPO1 serves as a major hub protein. To determine whether this nuclear export protein provides a target for radiosensitization, we defined the effects of the clinically relevant XPO1 inhibitor Selinexor on the radiosensitivity of glioblastoma cells. As determined by clonogenic survival analysis, Selinexor enhanced the radiosensitivity of GSCs but not normal fibroblast cell lines. Based on γ H2AX foci and neutral comet analyses, Selinexor inhibited the repair of radiation-induced DNA double strand breaks in GSCs suggesting that the Selinexor-induced radiosensitization is mediated by an inhibition of DNA repair. Consistent with a role for XPO1 in the nuclear to cytoplasm export of rRNA, Selinexor reduced 5S and 18S rRNA nuclear export in GSCs, which was accompanied by a decrease in gene translation efficiency, as determined from polysome profiles, as well as in protein synthesis. In contrast, rRNA nuclear export and protein synthesis were not reduced in normal cells treated with Selinexor. Orthotopic xenografts initiated from a GSC line were then used to define the in vivo response to Selinexor and radiation. Treatment of mice bearing orthotopic xenografts with Selinexor decreased tumor translational efficiency as determined from polysome profiles. Although Selinexor treatment alone had no effect on the survival of mice with brain tumors, it significantly enhanced the radiation-induced prolongation of survival. These results indicate that Selinexor enhances the radiosensitivity of glioblastoma cells and suggest that this effect involves a global inhibition of gene translation.

Keywords

radiation; XPO1; gene translation; glioblastoma stem-like cells; polysomes; Selinexor

Introduction

Radiotherapy continues to be a primary treatment modality for glioblastomas (GBMs). Although the delivery of radiation significantly contributes to the prolongation of patient survival, even in combination with surgery and chemotherapy, the median survival of

Corresponding author: Philip J. Tofilon, National Cancer Institute, 10 Center Drive-MSB 1002, Building 10, B3B69B, Bethesda, MD 20892, tofilonp@mail.nih.gov, Phone: (240) 858-3048.

Conflict of Interest: none

patients with GBM remains poor with the majority succumbing to disease within 16 months of diagnosis (1,2). Despite considerable migratory and invasive potential, pathological and imaging analyses have established that GBMs typically recur within the initial radiation treatment volume (3). This pattern of local failure indicates that GBM cells in situ are extremely radioresistant. Moreover, local recurrence suggests that the effectiveness of GBM therapy would benefit from the addition of a radiosensitizing agent. Towards this end, defining the molecular processes that mediate cellular radioresponse should provide a foundation for designing target based strategies that enhance GBM therapeutic response.

Genes whose expression is modified after irradiation have long been considered as a potential source of molecular targets for radiosensitization. Identifying such radiation-inducible genes has traditionally involved the analysis of total cellular mRNA, which defines the radiation-induced transcriptome. However, the poor correlation between the radiation-induced mRNAs and their corresponding proteins complicates the application of this approach to target identification (4). In contrast, analysis of polysome-bound mRNA bypasses the post-transcriptional events regulating gene expression to identify genes undergoing translation, which defines the radiation-induced translome (5–7). Comparisons of the transcriptomes and translomes from irradiated cells revealed few commonly affected genes, indicative of independent regulatory mechanisms. Moreover, in contrast to changes in the transcriptome, a strong correlation was detected between the mRNAs whose translational activity is affected by radiation and the expression of the corresponding proteins. These results suggested that analysis of radiation-induced translomes may provide unique information regarding the molecules that regulate cellular radioresponse.

To generate insight into the processes mediating the radioresponse of GBMs and to provide a potential source of molecular targets for radiosensitization, we recently used polysome gene expression profiling to define the radiation-induced translomes for a panel of human GBM stem-like cell (GSC) lines (7). Functional analysis of the radiation-induced translomes identified components of the DNA Damage Response, consistent with a role for translational control in cellular radioresponse, as well as other functions not typically associated with radioresponse such as cap-dependent translation and Golgi function. We have continued to mine the GSC radiation-induced translomes for genes associated with networks and processes that may be of functional significance with respect to radiosensitivity. Along these lines and as described herein, a network has been identified that regulates nucleus to cytoplasm transport. A major hub in this network is XPO1 (also referred to as CRM1), a critical nuclear transport receptor mediating the export of a subset of RNAs (8) as well as over 200 proteins (9,10), of which a number have implications in cancer biology. With respect to the potential of XPO1 to serve as a target for cancer treatment, small molecule inhibitors have recently been developed that specifically target XPO1 (11) with Selinexor (KPT-330) being the first to undergo clinical evaluation (12).

Selinexor was initially reported to have no effect on the radiosensitivity of primary GBM cell lines in vitro (13). However, in that study the evaluation of in vitro radiosensitivity was limited to measuring cell proliferation at 3 days after irradiation. More recently, a clonogenic assay was used to show that Selinexor enhanced the radiosensitivity of colorectal cancer cell lines (14). In the study described here, clonogenic analysis indicated that Selinexor enhanced

the radiosensitivity of GSC lines in vitro. Furthermore, this XPO1 inhibitor enhanced the radioresponse of orthotopic xenografts initiated from a GSC line. In both model systems, radiosensitization was associated with a decrease in general translational efficiency. These results suggest that Selinexor delivered in combination with radiotherapy may improve the effectiveness of GBM treatment.

Materials and Methods

Ingenuity Pathway Analysis

Microarray data previously described (7), available through GEO Series accession number GSE74084 was submitted to Ingenuity Pathway Analysis (QIAGEN, Redwood City,) for network analyses with IPA default settings and a p-value = 0.01 using pathway builder to visualize associations within a network.

Cell lines and treatments

Glioblastoma stem-like cell (GSC) lines NSC11 (provided by Dr. Frederick Lang, MD Anderson Cancer Center) and 0923, obtained from Neuro-Oncology Branch, NCI (15), were maintained as neurospheres in stem cell medium as described (7). CD133+ NSC11 (16,17) and CD15+ 0923 (18,19) cells were isolated from neurosphere cultures by FACS and used as a source for the described experiments. The CD133+ and CD15+ cell cultures met the criteria for tumor stem-like cells (16, 18). For use in an experiment, neurosphere cultures were disaggregated into single cells as described (17) and seeded onto poly-L-ornithine (Invitrogen)/laminin (Sigma) or for clonogenic assays, onto poly-L-lysine (Invitrogen) coated tissue culture plates. Under these conditions, single cell GSCs attach and proliferate maintaining their CD133+ or CD15+ expression and stem-like characteristics (20,21). NSC11 and 0923 cells were revived every 2 months from frozen stocks made after receiving cell lines and were most recently authenticated in May 2015, by STR analysis (Idexx Laboratories). U251 (glioblastoma) cells were obtained from the Division of Cancer Treatment and Diagnosis (DCTD) Tumor Repository, National Cancer Institute (NCI) and grown in DMEM/10% FBS. MRC5 and MRC9 (normal lung fibroblasts) were obtained from American Type Culture Collection and maintained in minimum essential medium with 10% FBS. Human astrocytes (ScienCell) were cultured according to company's protocol. All cells were cultured for less than 2 months after resuscitation from frozen stocks. Cell cultures were irradiated using a 320kV X-ray machine (Precision X Ray Inc.) at a dose rate of 2.3Gy/min; control cultures were mock irradiated. Selinexor (obtained from DCTD) was dissolved in dimethyl sulfoxide (DMSO) and used at 1 μ M based on previous studies (13,14).

Clonogenic Survival Assay

To evaluate radiosensitivity cells were plated at clonal density in six-well plates (cell numbers ranging from 25 to 8000 cells per well depending on cell line or radiation dose) and irradiated the next day. 10 to 18d after irradiation, plates were stained with 0.5% crystal violet, the number of colonies determined, and the surviving fractions were calculated. Radiation survival curves were generated after normalizing for the cytotoxicity induced by Selinexor.

Analysis of DNA damage

Visualization of γ H2AX foci was performed as previously described (7). The neutral comet assay was performed using a commercially available kit according to the manufacturer's instruction (Trevigen) and as described (16). Digital fluorescent images were analyzed with TriTek CometScore[®] (22). Data are expressed as % damage remaining in which the Olive tail moment from cultures irradiated on ice and collected immediately after irradiation was set to 100% damage, with the remaining times post-irradiation normalized accordingly. All time points were corrected for Selinexor or vehicle treatment alone by subtracting the Olive tail moment of sham irradiated vehicle or Selinexor treated samples. At least 50 cells per condition were measured.

Protein Synthesis Assay

Cells were plated in 24-well tissue culture plates in their respective media at a density of 3×10^4 cells per well and used in an experiment the next day. After treatment, media was removed and fresh media added containing O-propargyl-puromycin (OPP). After 0.5h, OPP detection and normalization to cell number was performed according to manufacturer instructions (Click-iT[™] Plus OPP Alexa Fluor[™] 488 Protein Synthesis Assay Kit, ThermoFisher).

Real-time RT-PCR

Total RNA was isolated from cytoplasmic and nuclear fractions using the PARIS[™] Kit (ThermoFisher) according to manufacturer's protocol. Complementary first-strand DNA was generated using the Applied Biosystems High-Capacity RNA-to-cDNA Kit. TaqMan assays for the specified genes (Applied Biosystems, ThermoFisher, 5S, Hs03682751_gH; 18S, Hs99999901_s1, ACTB, Hs99999903_m1), were used and PCR was performed using TaqMan RT-PCR kits (Applied Biosystems, ThermoFisher), according to the manufacturer's protocol. Relative fold changes in each fraction were determined by the C_t method using β -Actin as an internal control.

Orthotopic xenografts

CD133+ NSC11 cells (10^5) that had been engineered to express luciferase and GFP were orthotopically implanted into the right striatum of 6-week-old athymic female nude mice (NCr nu/nu; NCI Animal Production Program, Frederick, MD) as previously described (23). Bioluminescent imaging (BLI) and local irradiation were performed as described (16). On Day 24 post-implantation, mice were randomized according to the BLI signal into the four groups (7 mice/group), with treatments initiated the next day. Selinexor was dissolved in 0.6% Plasdone PVP K-29/32/0.6% Poloxamer Pluronic F-68 in sterile water (24). For irradiation, mice were anesthetized using a cocktail of ketamine/xylazine/acepromazine and placed in well-ventilated Plexi glass jigs with shielding of critical normal structures as described (20). Radiation was delivered using an XRad 320 X-irradiator (Precision X-Ray, Inc) at 320kV x-ray and a dose rate of 2.9Gy/min. Mice were monitored every day until the onset of neurologic symptoms (morbidity). GraphPad Prism 7, (GraphPad Software) was used to generate Kaplan–Meier survival curves, to calculate log-rank values, and to

determine one-way AVOVA of median survivals. All experiments were performed as approved by the principles and procedures in the NIH Guide for Care and Use of Animals.

Polysome Profiling

The procedure for polysome profiling of cells grown in vitro was performed as previously described (7). For polysome profiles from orthotopic NSC11 xenografts, mice were euthanized by CO₂ inhalation, brains rapidly removed and placed in PBS containing 100mg/mL cycloheximide. Tumors were then isolated based on GFP fluorescence under a stereoscope and flash frozen in liquid nitrogen. Approximately 20 mg of tumor was homogenized using a polytron in 0.9mL of lysis buffer (10mM Tris-HCl at pH 7.5, 150mM NaCl, 5mM MgCl₂, 500 U/mL RNasin [Promega]) supplemented to a final concentration of 1% deoxycholate and 1% Triton X-100 and left on ice for 10 minutes. Nuclei were removed by centrifugation (12,000g, 5min, at 4°C), and the supernatant was added to 500mL of extraction buffer (0.2M Tris-HCl at pH 7.5, 0.3M NaCl), 150 mg/mL cycloheximide, and 650 mg/mL heparin), and centrifuged (12,000g, 5min, at 4°C) to remove mitochondria and membranous debris. The supernatant was layered onto a 10mL linear sucrose gradient (10%–50% sucrose) [adapted from (25)] and centrifuged in a SW41Ti rotor (Beckman) at 35,000 × g for 3h at 4°C. Polysome profiles were then generated as described (7). Translational Efficiency (TE) was defined from a polysome profile as the area under the curve corresponding to polysome-bound RNA divided by the area corresponding to monosome-bound RNA plus polysome-bound RNA (26).

Results

As part of a previous study investigating the role of translational control of gene expression in cellular radioresponse, we defined the radiation-induced translome of the GSC line NSC11 (7). Functional analyses of this translome identified gene sets associated with the cellular processes of *DNA Damage Response*, *cap-dependent translation*, *Golgi function and mitochondrial oxidative phosphorylation* (7). Further interrogation of the NSC11 radiation-induced translome using Ingenuity Pathway Analysis (IPA) revealed an additional network associated with *nuclear-cytoplasmic transport*, which includes the GTPase RAN and its regulatory molecules as well as other molecules involved in nuclear export (Figure 1). The radiation-induced increase in the translational activity of these genes suggested that nuclear transport plays a role in determining the radiosensitivity of NSC11 cells. Of significance, although not in the radiation-induced translome (i.e., its translation was not affected by radiation), a hub molecule in this network is the critical nuclear export receptor XPO1 (27).

To test the hypothesis that nuclear export serves as a target for radiosensitization, NSC11 cells were treated with the combination of radiation and the XPO1 antagonist Selinexor and subjected to clonogenic survival analysis (Figure 2). Specifically, cells were plated at clonogenic density, allowed to attach overnight and Selinexor (1μM) added to culture media 1h before irradiation. 24h post-irradiation, cultures were rinsed and fresh, drug-free media was added with colonies determined 14 days later. As shown in Figure 2A, Selinexor enhanced NSC11 radiosensitivity with a dose enhancement factor (DEF) at a surviving fraction of 0.1 of 1.46. To determine whether the radiosensitization was unique to NSC11

cells, the same Selinexor/radiation treatment protocol was evaluated using the GSC line 0923. Exposure of the 0923 cells to Selinexor also resulted in an increase in radiosensitivity (DEF of 1.39). Selinexor treatment alone reduced the surviving fraction in NSC11 and 0923 cells (0.25 ± 0.01 and 0.68 ± 0.04 , respectively), which was normalized in the combination experiments. These data indicate that Selinexor enhances the radiosensitivity of GSCs. The same Selinexor treatment protocol was also evaluated using the long established GBM cell line U251 (Figure 2C). The XPO1 inhibitor enhanced the radiosensitivity of U251 cells with a DEF of 1.63 (determined at a surviving fraction of 0.15); treatment with Selinexor alone reduced survival to 0.27 ± 0.03 . These data indicate that Selinexor-induced radiosensitization is not limited to GSCs.

To gain insight into the mechanism through which Selinexor enhances GBM radiosensitivity, we focused on the GSC lines NSC11 and 0923. A previous study reported that the Selinexor-mediated radiosensitization of a rectal cancer cell line was due to an increase in apoptosis (14). Accordingly, apoptosis was evaluated in NSC11 and 0923 cells at 24h after 5Gy either with or without a 1h pre-treatment with Selinexor ($1\mu\text{M}$) (Figure S1). Consistent with previous results (23), radiation had no effect on apoptosis in either GSC line. Selinexor alone also did not affect the percentage of apoptotic cells; the combination of Selinexor and radiation had no effect of apoptosis as compared to vehicle treated cells. To further investigate the mechanism of Selinexor-induced radiosensitization, DSB repair was evaluated using γH2AX foci and neutral comet analyses. The level of radiation-induced DSBs corresponds to the number of γH2AX foci induced per cell whereas γH2AX dispersal correlates with DSB repair (28,29). Following the same protocol used in the clonogenic survival experiments, Selinexor ($1\mu\text{M}$) was added to culture media 1h before irradiation (2Gy) and γH2AX nuclear foci determined at times out to 24 hours (Figure 3A, Figure S2). No difference in foci levels was detected between control (vehicle) and Selinexor-treated cells up to 6h after irradiation, suggesting that Selinexor has no effect on the initial levels of radiation-induced DSBs. However, at 24h after irradiation, the number of γH2AX foci remaining was significantly greater in the Selinexor-treated cells than in control cells. The persistence of γH2AX foci in irradiated cells that were treated with Selinexor suggests an inhibition of DNA DSB repair. For the neutral comet assay, Selinexor was added to culture media 1h before exposure to 10Gy and cells collected for analysis at times out to 24h after irradiation (Figure 3B, Figure S2). For both cell lines, Selinexor treatment significantly slowed the repair of radiation-induced DSBs, which was detectable by 6h. The DSBs remaining at 24h reflect residual radiation-induced damage, which was increased in Selinexor-treated cells, and is consistent with an increase in radiation-induced cell death. Thus, data generated from the γH2AX and neutral comet assays suggest that Selinexor-induced radiosensitization involves the inhibition of DSB repair.

In addition to the export of a variety of proteins, XPO1 mediates the nuclear export of rRNA (30). To determine whether Selinexor affects rRNA nuclear export in the GSC lines, we used the approach of Castello et al (31) to quantitate the relative nuclear-cytoplasmic distribution of 5S and 18S rRNA (Figure 4A). Exposure of NSC11 and 0923 cells to Selinexor resulted in a decrease in cytoplasmic 5S and 18S rRNA and an increase in the rRNAs in the nucleus, consistent with an inhibition of nuclear rRNA export (31). These results suggest that Selinexor inhibits ribosomal biogenesis in the GSCs and may thus reduce gene translation.

Of note, Tabe et al reported that in lymphoma cell lines the XPO1 inhibitor KPT185 reduced the nuclear export of 50 ribosomal proteins suggesting an inhibition of ribosomal biogenesis (32). As an initial estimation of gene translation, translational efficiency (TE) was determined from polysome profiles generated from NSC11 and 0923 GSCs as a function of time after addition of Selinexor to the culture media. Representative profiles are shown in Figure 4B along with the TE values (the ratio of polysome-bound RNA to monosome-bound plus polysome-bound RNA (26)) from 3 independent experiments. The polysome fraction in both GSC lines was reduced beginning 1–6h after Selinexor treatment corresponding to a significant decrease in TE, which was further reduced after 24h of drug exposure. These results suggest that Selinexor disrupts gene translation. Of note, radiation was previously shown to have no effect on the polysome profile of NSC11 cells (33). Because the decrease in translational efficiency as calculated from polysome profiles suggest a corresponding decrease in protein synthesis, the *O*-propargyl-puromycin (OPP) assay was used to directly measure nascent protein production after Selinexor treatment (Figure 4C). Consistent with the polysome profiles, protein synthesis in NSC11 and 0923 cells was significantly reduced as early as 1h after Selinexor addition reaching a maximum reduction at 24h and 6h in NSC11 and 0923, respectively, levels comparable to cycloheximide treatment, which was used as a positive control. These data suggest that the Selinexor-mediated reduction in rRNA nuclear export leads to an inhibition of overall gene translation accompanied by the expected decrease in protein synthesis.

The clinical potential of a putative radiosensitizing agent will, in part, depend on its effects on the radiosensitivity of normal cells. Thus, the radiosensitivity of two normal fibroblast cell lines with and without Selinexor treatments were determined using the clonogenic survival assay. Following the same protocol used on tumor cells, MRC5 and MRC9 were plated to clonogenic density, allowed to attach overnight and treated with Selinexor (1 μ M) 1h before irradiation. 24h after irradiation cultures were rinsed and fresh, drug-free media added with colonies determined 15–18 days later. As shown in figure 5A, Selinexor had no effect on the radiosensitivity of MRC5 cells and appeared to slightly reduce the radiosensitivity of MRC9 cells. Selinexor exposure alone reduced the surviving fraction in both MRC5 and MRC9 to 0.26 ± 0.06 and 0.27 ± 0.02 , respectively. Along with the lack of radiosensitization, no change in protein synthesis was detected in the fibroblasts out to 24h of Selinexor exposure (Figure 5B). As a normal cell that is more directly relevant to CNS radioresponse, human astrocytes were also evaluated. Although normal astrocytes do not form colonies, which eliminates clonogenic survival analysis, protein synthesis can be measured. As for normal fibroblasts, Selinexor treatment out to 24h had no effect on protein synthesis in astrocytes. Thus, in contrast to the GBM cell lines, Selinexor had no effect on protein synthesis in the normal cells evaluated. Analysis of 5S and 18S rRNA nuclear-cytoplasmic distribution after Selinexor treatment of the normal cell lines is shown in Figure 5C. Selinexor treatment of MRC5 cells induced a slight, but significant decrease in both cytoplasmic and nuclear 18S; no significant changes in 5S were detected. In MRC9 and astrocytes no significant changes were detected in 5S or 18S nuclear-cytoplasmic distribution after Selinexor exposure. Importantly, the absence of an increase in nuclear 5S and 18S rRNA suggests that rRNA export was not inhibited by Selinexor in these normal cells. The tumor cell selectivity of Selinexor with respect to the inhibition of rRNA export

and protein synthesis as well as radiosensitization may involve XPO1 protein expression. As shown (Figure S3), XPO1 expression is greater in the 3 GBM cell lines as compared to the normal cells. It has been previously reported that, although Selinexor inhibits XPO1 activity (11), it has no effect on the XPO1 expression level in GBM cells (13).

Finally, to evaluate the potential of Selinexor to enhance GBM radiosensitivity under in vivo conditions, we used orthotopic xenografts initiated from NSC11 cells. In vitro results suggested that protein synthesis provides a marker of Selinexor radiosensitizing activity. Whereas it is not possible to directly measure protein synthesis in brain tumors using the OPP assay, polysome profiles can be generated and translational efficiency (TE) determined. Towards this end, mice bearing NSC11 brain tumors (40days post-implantation) were treated with a single dose of Selinexor (20mg/kg); tumors were collected at times out to 48h and polysome profiles generated from individual tumors. Representative profiles are shown in figure 6A along with the TEs (mean \pm SEM) generated from 3 mice. As reflected by the reduction in polysome fraction, TE was decreased by 1h after Selinexor administration reaching a maximum reduction by approximately 24h, which appeared to begin to recover towards untreated levels at 48h. These results indicate that Selinexor penetrates the blood-brain barrier and suggests that it targets the same processes within the tumor as detected in vitro. Based on the time course of the TE decrease, a protocol was designed to test the antitumor effectiveness the Selinexor/radiation combination. At 24 days after intracerebral implant mice were randomized according to BLI signal into 4 groups: vehicle (control), radiation (2Gy), Selinexor (20 mg/kg), and Selinexor plus radiation. Radiation was delivered daily for 5 days (5 \times 2Gy) with Selinexor delivered on days 1, 3, and 5, 1h prior to local irradiation. Mice were followed until the initial onset of morbidity and survival curves generated. Selinexor treatment of mice alone had no significant effect on survival as compared to vehicle; radiation alone resulted in a significant increase in survival (Figure 6B). The survival of mice receiving the combination protocol was significantly increased as compared with control and, importantly, as compared with radiation alone. The median survival times for the treatment groups are shown in the boxplots in Figure 6C. Whereas the median survival after Selinexor was not significantly different from vehicle, radiation alone increased median survival by 9 days and the combination by 18 days versus vehicle, indicating that the combination protocol increased tumor radiosensitivity with an apparent DEF of 2. Of note, no excessive weight loss was detected in mice receiving Selinexor/radiation combination protocol (Figure S4). Thus, these data suggest that Selinexor inhibits gene translation in orthotopic brain tumors and enhances their radiosensitivity.

Discussion

The data presented here indicate that the XPO1 inhibitor Selinexor enhances the radiosensitivity of GBM cells. These results are in contrast to the report by Green et al (13), who initially proposed the use on XPO1 inhibitors for the treatment of GBM. In their study, the evaluation of in vitro radiosensitivity of primary GBM cell lines was limited to measuring cell proliferation in a 96-well format 3days after completion of fractionated irradiation. Whether the conflicting results can be attributed to different cell lines and/or experimental analysis of radiosensitivity (short-term proliferation versus clonogenicity) is unclear. However, in a more recent study Ferreiro-Neira et al, using a clonogenic assay

reported that Selinexor enhances the in vitro radiosensitivity of colorectal tumor cells (14). Given that clonogenic analysis is the gold standard for defining radiosensitivity, it appears that Selinexor does have radiosensitizing activity, which is not restricted to a specific tumor cell type.

The anti-cancer actions of Selinexor have been generally attributed to a reduction in the nucleus to cytoplasm transport of critical tumor suppressor and/or oncogenic proteins (10,27,34,35). With respect to the Selinexor-mediated radiosensitization of colorectal tumor cells, the mechanism proposed involved the prevention of survivin export into the cytoplasm, which resulted in an increase in apoptotic cell death (14). For GSCs, no change in apoptosis after Selinexor, irradiation or the combination was detected suggesting that proteins regulating apoptosis are not involved in their radiosensitization and suggests an additional mechanism for radiosensitization of GSCs. Given the number of proteins transported by XPO1, Selinexor could enhance radiosensitivity through a number of independent mechanisms in a cell type dependent manner. However, because XPO1 regulates nuclear export of ribosomal RNA (36) as well as ribosomal proteins (32,37), its inhibition would likely affect the general process of gene translation. Supporting this hypothesis, Selinexor was shown here to inhibit rRNA nuclear export in the GSC lines. Moreover, translational efficiency, indicative of mRNA undergoing active translation (26), was reduced after Selinexor treatment of glioma cells grown in vitro and as orthotopic xenografts. Of note, consistent with an inhibition of rRNA nuclear export, in each set of polysome profiles Selinexor treatment resulted in a slight decrease in the 40S and/or 60S monosome peaks along with the reduction in polysomes suggesting a decrease in cytoplasmic rRNA. Importantly, the Selinexor-mediated inhibition of translation in vitro was validated by the OPP incorporation assay, which directly measures protein synthesis. We have previously reported that inhibiting translation via reducing mTOR activity (23,38) and eIF4E levels (39) enhanced tumor cell radiosensitivity and inhibited DSB repair. The results presented here suggest that the inhibition of translation plays a role in the Selinexor-induced radiosensitization of GBM cells.

Consistent with a role for translation inhibition in mediating Selinexor-induced radiosensitization of tumor cells, the XPO1 inhibitor had no effect on protein synthesis in normal cell lines. However, whereas Selinexor had no effect on protein synthesis in normal cells, it did induce a significant level of cytotoxicity, which was similar to that induced in tumor cells. This suggests that the radiosensitization and cytotoxicity that result from XPO1 inhibition occur via different mechanisms. Alternatively, this may also reflect the dysregulation of translation (32) and/or nuclear-cytoplasmic transport (10,12,24,27) in tumor cells. Along these lines, XPO1 is overexpressed in GBM (40,41), which is consistent with the data herein showing that XPO1 protein levels are greater in the GBM cell lines as compared to normal fibroblasts and astrocytes. Regardless of the mechanisms involved, the data suggest that whereas the cytotoxicity induced by Selinexor is not limited to tumor cells, this XPO1 inhibitor induces tumor selective radiosensitization.

In the initial preclinical study of Selinexor as a potential GBM treatment, Green et al reported pharmacokinetics indicative of penetrating the blood-brain barrier and showed reduced XPO1 protein levels in brain tumor xenografts (13). Moreover, they showed that for

mice bearing orthotopic GBM xenografts, a Selinexar treatment protocol of 3× week until morbidity resulted in a significant prolongation of survival as compared to vehicle-treated animals. Using polysome profiling, we showed that a single dose of Selinexar inhibits translation in orthotopic brain tumors, which was detectable at 1h and continued for 24h before beginning to return to control at 48h. When Selinexar was given every other day for only a week no effect on animal survival was detected. This lack of an effect as compared to the previous report is likely due to the relatively short Selinexar treatment period. However, this same Selinexar treatment protocol, which was designed to maintain the translation inhibition over the 5day fractionated irradiation schedule, resulted in a significant increase in the radiation-induced prolongation of animal survival, indicative of in vivo radiosensitization. Thus, given that Selinexar is already in clinical trials, these data suggest that delivery of this XPO1 inhibitor in combination with radiotherapy may improve GBM treatment response.

Supplementary Material

Refer to Web version on PubMed Central for supplementary material.

Acknowledgments

Financial Support: Division of Basic Sciences, Intramural Program, National Cancer Institute (Z1ABC011372, Z1ABC011373) to P.J. Tofilon.

References

1. Berkey FJ. Managing the adverse effects of radiation therapy. *Am Fam Physician*. 2010; 82:381–8. 94. [PubMed: 20704169]
2. Liauw SL, Connell PP, Weichselbaum RR. New paradigms and future challenges in radiation oncology: an update of biological targets and technology. *Sci Transl Med*. 2013; 5:173sr2. [PubMed: 23427246]
3. Hochberg FH, Pruitt A. Assumptions in the radiotherapy of glioblastoma. *Neurology*. 1980; 30:907–11. [PubMed: 6252514]
4. Szkanderova S, Port M, Stulik J, Hernychova L, Kasalova I, Van Beuningen D, et al. Comparison of the abundance of 10 radiation-induced proteins with their differential gene expression in L929 cells. *Int J Radiat Biol*. 2003; 79:623–33. [PubMed: 14555345]
5. Harding HP, Novoa I, Zhang Y, Zeng H, Wek R, Schapira M, et al. Regulated translation initiation controls stress-induced gene expression in mammalian cells. *Mol Cell*. 2000; 6:1099–108. [PubMed: 11106749]
6. Kumaraswamy S, Chinnaiyan P, Shankavaram UT, Lu X, Camphausen K, Tofilon PJ. Radiation-induced gene translation profiles reveal tumor type and cancer-specific components. *Cancer Res*. 2008; 68:3819–26. [PubMed: 18483266]
7. Wahba A, Rath BH, Bisht K, Camphausen K, Tofilon PJ. Polysome profiling links translational control to the radioresponse of glioblastoma stem-like cells. *Cancer Res*. 2016
8. Okamura M, Inose H, Masuda S. RNA Export through the NPC in Eukaryotes. *Genes (Basel)*. 2015; 6:124–49. [PubMed: 25802992]
9. Fukuda M, Asano S, Nakamura T, Adachi M, Yoshida M, Yanagida M, et al. CRM1 is responsible for intracellular transport mediated by the nuclear export signal. *Nature*. 1997; 390:308–11. [PubMed: 9384386]
10. Xu D, Grishin NV, Chook YM. NESdb: a database of NES-containing CRM1 cargoes. *Mol Biol Cell*. 2012; 23:3673–6. [PubMed: 22833564]

11. Neggers JE, Vercruyse T, Jacquemyn M, Vanstreels E, Baloglu E, Shacham S, et al. Identifying drug-target selectivity of small-molecule CRM1/XPO1 inhibitors by CRISPR/Cas9 genome editing. *Chem Biol.* 2015; 22:107–16. [PubMed: 25579209]
12. Abdul Razak AR, Mau-Soerensen M, Gabrail NY, Gerecitano JF, Shields AF, Unger TJ, et al. First-in-Class, First-in-Human Phase I Study of Selinexor, a Selective Inhibitor of Nuclear Export, in Patients With Advanced Solid Tumors. *J Clin Oncol.* 2016; 34:4142–50. [PubMed: 26926685]
13. Green AL, Ramkissoon SH, McCauley D, Jones K, Perry JA, Hsu JH, et al. Preclinical antitumor efficacy of selective exportin 1 inhibitors in glioblastoma. *Neuro Oncol.* 2015; 17:697–707. [PubMed: 25366336]
14. Ferreiro-Neira I, Torres NE, Liesenfeld LF, Chan CH, Penson T, Landesman Y, et al. XPO1 Inhibition Enhances Radiation Response in Preclinical Models of Rectal Cancer. *Clin Cancer Res.* 2016; 22:1663–73. [PubMed: 26603256]
15. Ene CI, Edwards L, Riddick G, Baysan M, Woolard K, Kotliarova S, et al. Histone demethylase Jumonji D3 (JMJD3) as a tumor suppressor by regulating p53 protein nuclear stabilization. *PLoS One.* 2012; 7:e51407. [PubMed: 23236496]
16. Jamal M, Rath BH, Tsang PS, Camphausen K, Tofilon PJ. The brain microenvironment preferentially enhances the radioresistance of CD133(+) glioblastoma stem-like cells. *Neoplasia.* 2012; 14:150–8. [PubMed: 22431923]
17. McCord AM, Jamal M, Williams ES, Camphausen K, Tofilon PJ. CD133+ glioblastoma stem-like cells are radiosensitive with a defective DNA damage response compared with established cell lines. *Clin Cancer Res.* 2009; 15:5145–53. [PubMed: 19671863]
18. Nevo I, Woolard K, Cam M, Li A, Webster JD, Kotliarov Y, et al. Identification of molecular pathways facilitating glioma cell invasion in situ. *PLoS One.* 2014; 9:e111783. [PubMed: 25365423]
19. Son MJ, Woolard K, Nam DH, Lee J, Fine HA. SSEA-1 is an enrichment marker for tumor-initiating cells in human glioblastoma. *Cell Stem Cell.* 2009; 4:440–52. [PubMed: 19427293]
20. Pollard SM, Yoshikawa K, Clarke ID, Danovi D, Stricker S, Russell R, et al. Glioma stem cell lines expanded in adherent culture have tumor-specific phenotypes and are suitable for chemical and genetic screens. *Cell Stem Cell.* 2009; 4:568–80. [PubMed: 19497285]
21. Rath BH, Fair JM, Jamal M, Camphausen K, Tofilon PJ. Astrocytes enhance the invasion potential of glioblastoma stem-like cells. *PLoS One.* 2013; 8:e54752. [PubMed: 23349962]
22. Collins AR. The comet assay for DNA damage and repair: principles, applications, and limitations. *Mol Biotechnol.* 2004; 26:249–61. [PubMed: 15004294]
23. Kahn J, Hayman TJ, Jamal M, Rath BH, Kramp T, Camphausen K, et al. The mTORC1/mTORC2 inhibitor AZD 2014 enhances the radiosensitivity of glioblastoma stem-like cells. *Neuro Oncol.* 2014; 16:29–37. [PubMed: 24311635]
24. Kim J, McMillan E, Kim HS, Venkateswaran N, Makkar G, Rodriguez-Canales J, et al. XPO1-dependent nuclear export is a druggable vulnerability in KRAS-mutant lung cancer. *Nature.* 2016; 538:114–7. [PubMed: 27680702]
25. del Prete MJ, Vernal R, Dolznig H, Mullner EW, Garcia-Sanz JA. Isolation of polysome-bound mRNA from solid tissues amenable for RT-PCR and profiling experiments. *RNA.* 2007; 13:414–21. [PubMed: 17237355]
26. Koritzinsky M, Magagnin MG, van den Beucken T, Seigneuric R, Savelkoul K, Dostie J, et al. Gene expression during acute and prolonged hypoxia is regulated by distinct mechanisms of translational control. *EMBO J.* 2006; 25:1114–25. [PubMed: 16467844]
27. Cook A, Bono F, Jinek M, Conti E. Structural biology of nucleocytoplasmic transport. *Annu Rev Biochem.* 2007; 76:647–71. [PubMed: 17506639]
28. Bonner WM, Redon CE, Dickey JS, Nakamura AJ, Sedelnikova OA, Solier S, et al. GammaH2AX and cancer. *Nat Rev Cancer.* 2008; 8:957–67. [PubMed: 19005492]
29. Lobrich M, Shibata A, Beucher A, Fisher A, Ensminger M, Goodarzi AA, et al. gammaH2AX foci analysis for monitoring DNA double-strand break repair: strengths, limitations and optimization. *Cell Cycle.* 2010; 9:662–9. [PubMed: 20139725]
30. Kohler A, Hurt E. Exporting RNA from the nucleus to the cytoplasm. *Nat Rev Mol Cell Biol.* 2007; 8:761–73. [PubMed: 17786152]

31. Castello A, Izquierdo JM, Welnowska E, Carrasco L. RNA nuclear export is blocked by poliovirus 2A protease and is concomitant with nucleoporin cleavage. *J Cell Sci.* 2009; 122:3799–809. [PubMed: 19789179]
32. Tabe Y, Kojima K, Yamamoto S, Sekihara K, Matsushita H, Davis RE, et al. Ribosomal Biogenesis and Translational Flux Inhibition by the Selective Inhibitor of Nuclear Export (SINE) XPO1 Antagonist KPT-185. *PLoS One.* 2015; 10:e0137210. [PubMed: 26340096]
33. Wahba A, Lehman SL, Tofilon PJ. Radiation-induced translational control of gene expression. *Translation (Austin).* 2017; 5:e1265703. [PubMed: 28702276]
34. Kau TR, Way JC, Silver PA. Nuclear transport and cancer: from mechanism to intervention. *Nat Rev Cancer.* 2004; 4:106–17. [PubMed: 14732865]
35. Turner JG, Marchion DC, Dawson JL, Emmons MF, Hazlehurst LA, Washausen P, et al. Human multiple myeloma cells are sensitized to topoisomerase II inhibitors by CRM1 inhibition. *Cancer Res.* 2009; 69:6899–905. [PubMed: 19690141]
36. Siddiqui N, Borden KL. mRNA export and cancer. *Wiley Interdiscip Rev RNA.* 2012; 3:13–25. [PubMed: 21796793]
37. Sengupta J, Bussiere C, Pallesen J, West M, Johnson AW, Frank J. Characterization of the nuclear export adaptor protein Nmd3 in association with the 60S ribosomal subunit. *J Cell Biol.* 2010; 189:1079–86. [PubMed: 20584915]
38. Hayman TJ, Wahba A, Rath BH, Bae H, Kramp T, Shankavaram UT, et al. The ATP-competitive mTOR inhibitor INK128 enhances in vitro and in vivo radiosensitivity of pancreatic carcinoma cells. *Clin Cancer Res.* 2014; 20:110–9. [PubMed: 24198241]
39. Hayman TJ, Williams ES, Jamal M, Shankavaram UT, Camphausen K, Tofilon PJ. Translation initiation factor eIF4E is a target for tumor cell radiosensitization. *Cancer Res.* 2012; 72:2362–72. [PubMed: 22397984]
40. Liu X, Chong Y, Tu Y, Liu N, Yue C, Qi Z, et al. CRM1/XPO1 is associated with clinical outcome in glioma and represents a therapeutic target by perturbing multiple core pathways. *J Hematol Oncol.* 2016; 9:108. [PubMed: 27733172]
41. Shen A, Wang Y, Zhao Y, Zou L, Sun L, Cheng C. Expression of CRM1 in human gliomas and its significance in p27 expression and clinical prognosis. *Neurosurgery.* 2009; 65:153–9. discussion 9–60. [PubMed: 19574837]

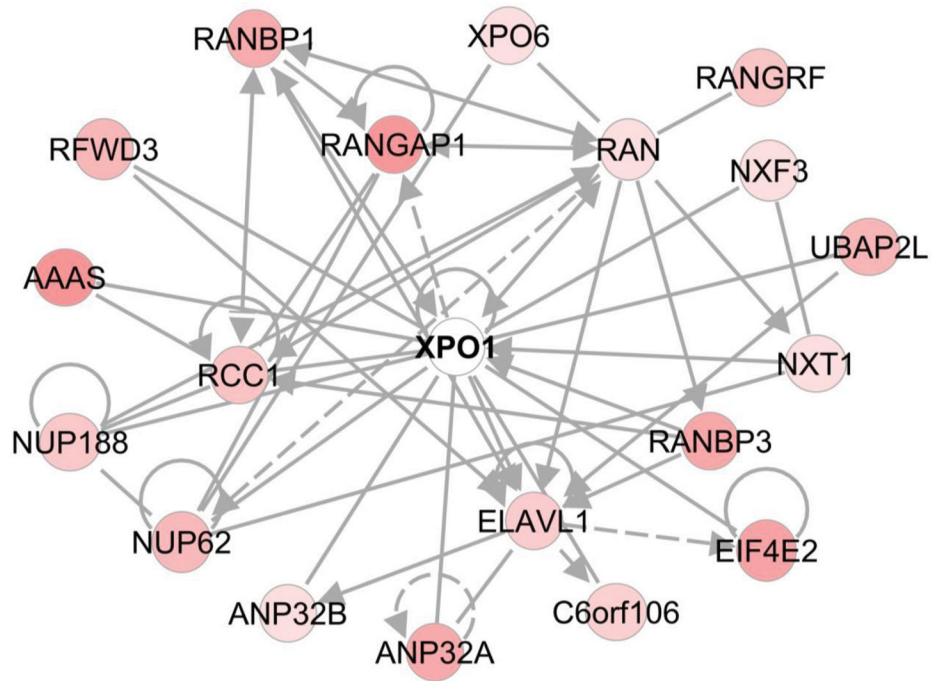


Figure 1. IPA network of genes in the radiation-induced transcriptome of NSC11 cells involved in nuclear export. Genes up-regulated are in pink (intensity of color is descriptive of the level of up-regulation).

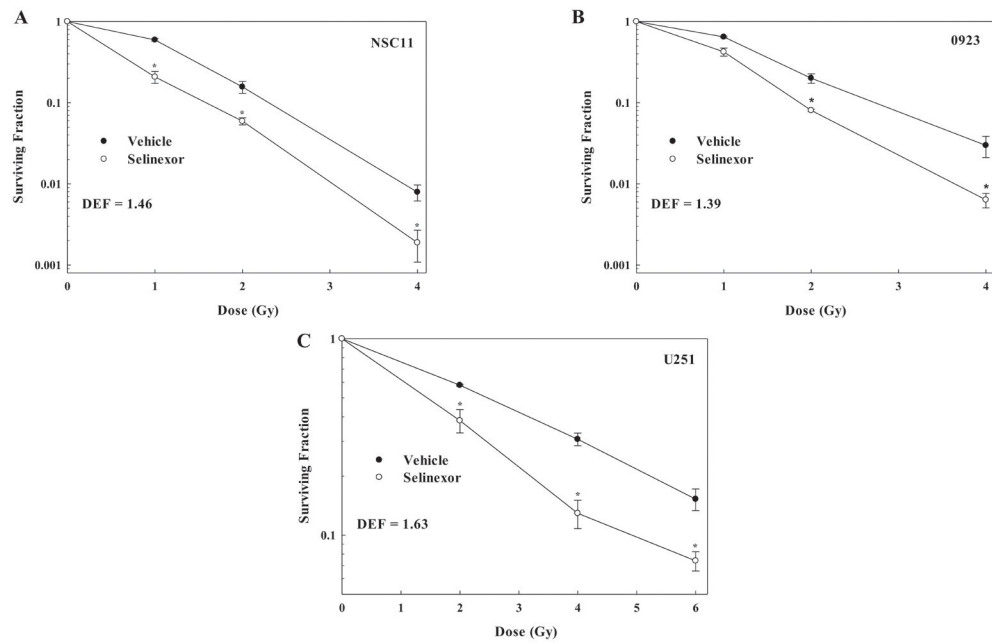


Figure 2. Effect of Selinexor on the in vitro radiosensitivity of GBM cells. **A)** NSC11 **B)** 0923 and **C)** U251 cells. Selinexor (1 μ M) or vehicle (DMSO) were added to culture media 1h before irradiation; 24h later media was replaced with fresh, drug-free media and colonies determined after 10–14 days. Dose enhancement factors (DEFs) were calculated at a surviving fraction of 0.1 or for U251 at 0.15. Values represent the mean \pm SEM of 3 independent experiments. * $p < 0.05$, Student's t -test (Selinexor vs. Vehicle).

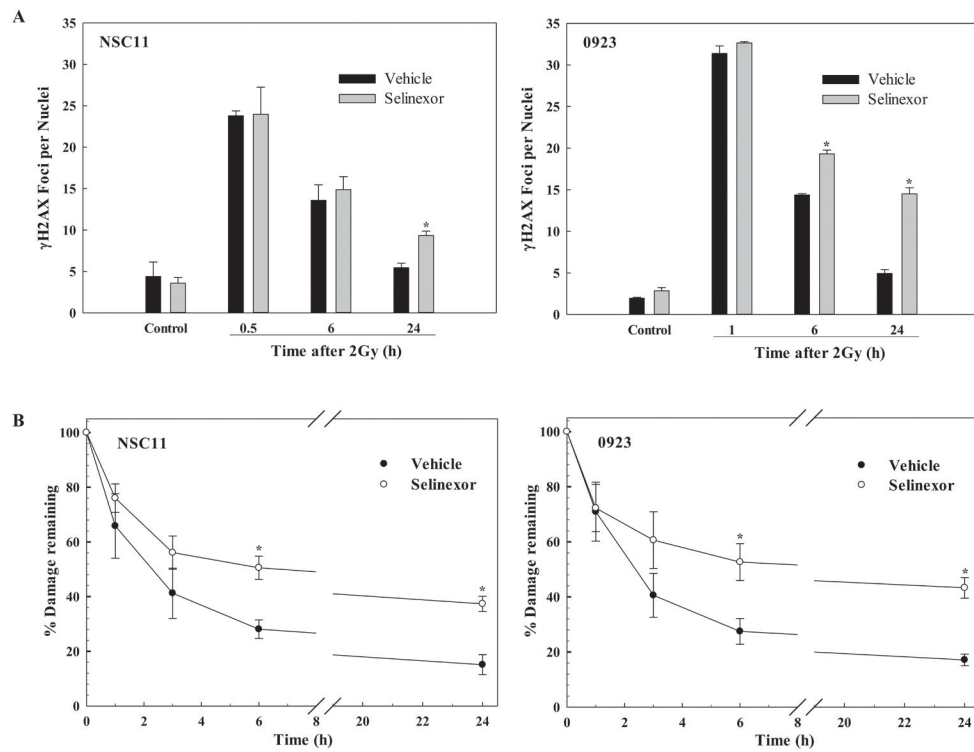


Figure 3. Influence of Selinexor on radiation-induced DNA damage in NSC11 and 0923 cells. **A)** γ H2AX foci analysis. Selinexor ($1\mu\text{M}$) was added to cultures 1h prior to irradiation (2Gy) and cells collected at the designated time points for γ H2AX foci analysis. γ H2AX foci were counted in 25 cells per experiment without knowledge of the treatment. For unirradiated groups, vehicle or Selinexor exposure was for 24h. Values represent the mean \pm SEM of 3 independent experiments. **B)** Neutral comet assay. Cells were irradiated (10Gy) and analyzed at times out to 24h. Data are expressed as percent damage remaining in which the tail moment immediately after radiation corresponds to 100% damage. Values represent the mean \pm SEM of 3 independent experiments. * $p < 0.05$, Student's t -test (Selinexor vs. Vehicle).

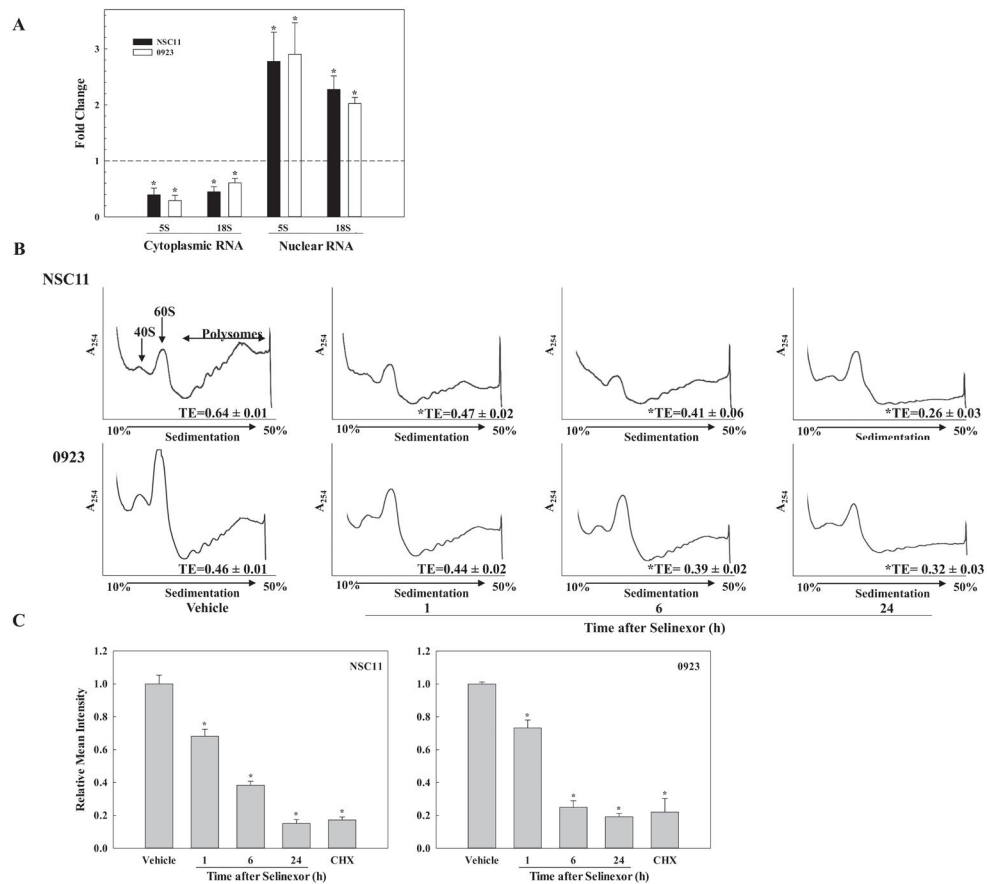
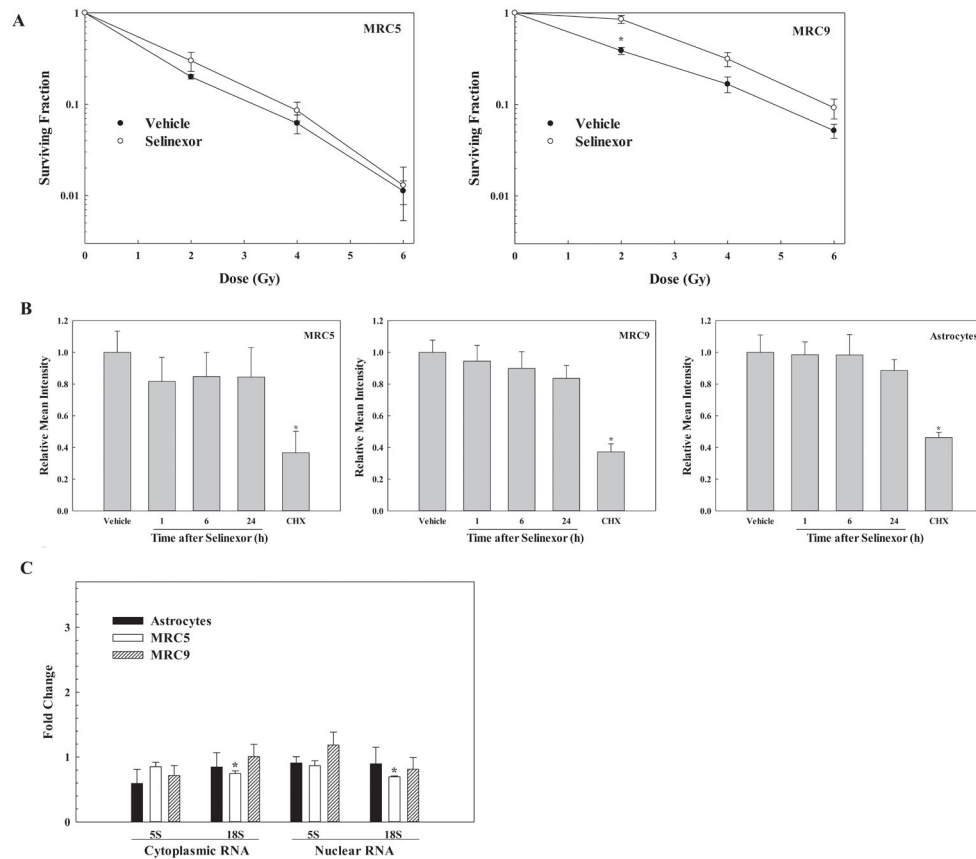


Figure 4. rRNA nuclear export, translational efficiency and protein synthesis in GSCs treated with Selinexor. **A)** rRNA nuclear-cytoplasmic distribution after Selinexor treatment of NSC11 and 0923 cells. Cultures were exposed to vehicle or Selinexor (1 μ M, 24h) and the levels of 5S and 18S rRNA transcripts in cytoplasmic and nuclear fractions determined. Values were normalized to β -Actin mRNA in each compartment with vehicle-treated cells set to 1.0 (dashed line) for calculation of fold-change. Values represent the mean \pm SEM of 3 independent experiments. **B)** Representative polysome profiles of NSC11 (top) and 0923 (bottom) cells as a function of time after Selinexor (1 μ M) addition to media. Translational efficiency (TE) values represent the mean \pm SEM of 3 independent experiments. **C)** Protein synthesis as measured by OPP incorporation as a function of time after Selinexor (1 μ M) addition to media for NSC11 (left) and 0923 (right). Cycloheximide (CHX, 0.25 μ M, 4h) was used as a positive control for protein synthesis inhibition. Values represent the mean \pm SEM of 3 independent experiments. * $p < 0.05$, Student's t -test (Selinexor vs. Vehicle).

**Figure 5.**

The effect of Selinexor on normal cell the radiosensitivity, protein synthesis and rRNA nuclear export. A) Radiosensitivity of normal cell lines MRC5 (left) and MRC9 (right). Selinexor (1 μ M) or vehicle (DMSO) were added to culture media 1h before irradiation; 24h later fresh, drug-free media was added and colonies determined 14 days later. B) Protein synthesis as measured by OPP incorporation as a function of time after Selinexor (1 μ M) addition to media for MRC5 (left), MRC9 (middle), and astrocytes (right). Cycloheximide (CHX, 0.25 μ M, 4h) was used as a positive control for protein synthesis inhibition. C) rRNA nuclear-cytoplasmic distribution after Selinexor treatment of MRC5, MRC9, and astrocytes. Cells were exposed to vehicle or Selinexor (1 μ M, 24h) and the levels of 5S and 18S rRNA transcripts in cytoplasmic and nuclear compartments were determined. Values were normalized to β -Actin mRNA and vehicle-treated cells set to 1.0 (dashed line) for calculation of fold-change. All values represent the mean \pm SEM of 3 independent experiments. * $p < 0.05$, Student's *t*-test (Selinexor vs. Vehicle).

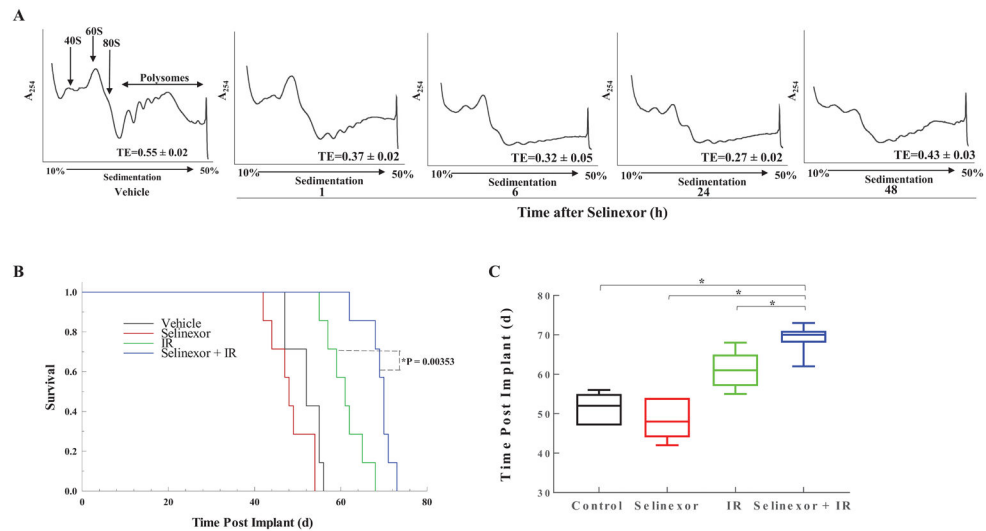


Figure 6. The effect of Selinexor on (A) translational efficiency and (B, C) radioresponse of NSC11-initiated orthotopic xenograft. (A) Mice bearing orthotopic xenografts (40 days after implant, before the onset of morbidity) were treated with vehicle or Selinexor (20mg/kg) by oral gavage. Tumors were collected at the indicated timepoints and polysome profiles generated. Representative profiles from each treatment group are shown; Translational efficiency (TE) values represent the mean \pm SEM of 3 mice. Student's t-test, * p 0.05, Student's t-test, Selinexor v. Vehicle. (B) At 24 days after orthotopic implant, mice were randomized and treatment initiated the following day as described in text (IR= 5 \times 2Gy). Kaplan-Meier survival curves were generated with log-rank analysis for comparison. (C) Box plot graph of median survival of each treatment group, * p < 0.05, by Dunnett's multiple comparison test.